

# Platelet-Derived Growth Factor Preserves Retinal Synapses in a Rat Model of Ocular Hypertension

Rachel S. Chong,<sup>1-4</sup> Andrew Osborne,<sup>4</sup> Raquel Conceição,<sup>4</sup> and Keith R. Martin<sup>4-7</sup>

<sup>1</sup>Singapore National Eye Centre, Singapore

<sup>2</sup>Singapore Eye Research Institute, Singapore

<sup>3</sup>Agency for Science, Technology and Research, Singapore

<sup>4</sup>John van Geest Centre for Brain Repair, University of Cambridge, Cambridge, United Kingdom

<sup>5</sup>Wellcome Trust Medical Research Council Cambridge Stem Cell Institute, Cambridge, United Kingdom

<sup>6</sup>Cambridge NIHR Biomedical Research Centre, Cambridge, United Kingdom

<sup>7</sup>Eye Department, Addenbrooke's Hospital, Cambridge, United Kingdom

Correspondence: Keith R. Martin, John van Geest Centre for Brain Repair, University of Cambridge, E.D. Adrian Building, Forvie Site, Robinson Way, Cambridge, CB2 0PY, UK; krgm2@cam.ac.uk.

Submitted: August 3, 2015

Accepted: January 25, 2016

Citation: Chong RS, Osborne A, Conceição R, Martin KR. Platelet-derived growth factor preserves retinal synapses in a rat model of ocular hypertension. *Invest Ophthalmol Vis Sci*. 2016;57:842-852. DOI:10.1167/iops.15-17864

**PURPOSE.** Platelet-derived growth factor (PDGF) promotes neuronal survival in experimental glaucoma and recruits glial cells that regulate synapses. We investigated the effects of intravitreal PDGF on the inflammatory milieu and retinal synapses in the presence of raised IOP.

**METHODS.** Animals with laser-induced IOP elevation received intravitreal injections of either saline or 1.5 µg PDGF. At 7 days, a further intravitreal injection was administered so groups received "PDGF-saline" ( $n = 15$ ), "PDGF-PDGF" ( $n = 13$ ), or "saline-saline" ( $n = 20$ ). Platelet-derived growth factor receptor activation was assessed after 2 weeks using Western blot for PI3 kinase. Immunohistochemistry was performed for markers of synapses in the inner plexiform layer (IPL): PSD-95, GluR1, SY38; RGCs:  $\beta$ III-tubulin, and glial cells: Iba-1, CD45. Real-time quantitative polymerase chain reaction (qPCR) was performed for *Arc*, *seip*, *MCP-1*, *IL-6*, *IL-10*, and *CX3CR1* ( $n = 13$ ).

**RESULTS.** A single injection of PDGF increased IPL synaptic density in high IOP eyes (PSD-95 =  $8.65 \pm 0.43$ , SY38 =  $8.68 \pm 0.51$ , GluR1 =  $9.03 \pm 0.60$  puncta/ $\mu\text{m}^3$ ,  $P < 0.001$ ) and expression of synaptic modulator *Arc* ( $6.92 \pm 3.71$ -fold change/control,  $P < 0.05$ ) in comparison with vehicle (PSD-95 =  $4.59 \pm 0.41$ , SY38 =  $4.46 \pm 0.38$ , GluR1 =  $5.94 \pm 0.50$  puncta/ $\mu\text{m}^3$ , *Arc* =  $1.46 \pm 0.31$ -fold/change/control). This was associated with more resident microglia ( $8.16 \pm 1.34$ -fold change/control,  $P < 0.001$ ) and infiltrating monocyte-derived macrophages in the retina as well as increased *Seip* expression ( $26.8 \pm 14.12$ -fold change/control,  $P < 0.05$ ). Optic nerve head (ONH) showed an increased microglia (saline =  $1.44 \pm 0.13$  versus PDGF =  $2.23 \pm 0.18$ -fold change/control,  $P < 0.01$ ) but not infiltrating macrophages. *IL-10* expression was significantly increased in PDGF-treated eyes ( $5.43 \pm 0.47$ -fold change/control,  $P < 0.05$ ) relative to vehicle ( $2.51 \pm 0.67$ -fold change/control).

**CONCLUSIONS.** Platelet-derived growth factor increased microglial and monocyte-derived macrophage populations in the eye and protected intraretinal synapses from degeneration in our experimental glaucoma model.

Keywords: synapses, macrophages, glaucoma posterior segment

Platelet-derived growth factor (PDGF) is an important mediator of the neuroprotective effect of mesenchymal stem cells on retinal ganglion cells (RGCs) in retinal explants as well as in experimental glaucoma.<sup>1</sup> Platelet-derived growth factor also appears to enhance neuronal survival in a number of other injury models including excitotoxicity<sup>2</sup> and oxidative stress.<sup>3</sup>

Platelet-derived growth factor may promote RGC survival through a direct effect on the PI3 kinase/AKT pathway that prevents cell death.<sup>4,5</sup> However, it also is a potent chemoattractant and activator of inflammatory cells which modulate neuronal health throughout the central nervous system (CNS).<sup>6-8</sup> Platelet-derived growth factor has a particularly marked effect on microglial proliferation and monocyte transmigration in the CNS via monocyte-chemoattractant protein 1.<sup>9</sup>

Microglia regulate synapses in development and disease,<sup>10-12</sup> via intimate contact between their filopodia and dendritic spines in the CNS.<sup>13</sup> Early microglial activation has been noted in experimental models of glaucoma,<sup>14,15</sup> while a growing body of evidence also suggests that synaptic loss is an initial feature of glaucoma that occurs before signs of RGC death<sup>16,17</sup> or changes to the dendritic structure<sup>18</sup> are observed.

We have shown previously that intravitreally-administered PDGF protects against loss of RGC bodies and axons in an experimental model of glaucoma.<sup>1</sup> However, effective RGC neuroprotection also requires protection of the dendritic compartment and the effect of PDGF on RGC dendrites and synapses within the retina is unknown. Given the known effects of PDGF on microglia and the role of microglia in synaptic regulation in development and disease, we hypothe-



sized that PDGF treatment may modulate the effect of IOP on retinal dendrites and synapses in a rat model with raised IOP. We measured RGC survival and dendrite health using  $\beta$ III-tubulin immunostaining, and analysed the retina for changes in synaptic markers, such as postsynaptic density 95 (PSD-95), glutamate receptor-1 (GluR1), as well as synaptophysin 38 (SY38). Microglia and monocyte-derived macrophage populations in the retina and optic nerve head (ONH) were assessed based on Iba-1 and differential CD45 expression. Gene expression of *Arc*, which regulates synapses in the CNS, the chemokine receptor *CX3CR1*, and inflammatory cytokines *IL-10* and *IL-6*, also were measured with real time polymerase chain reaction (qPCR).

We report for the first time to our knowledge that PDGF protects intraretinal synapses and dendrites from degeneration in eyes with experimental IOP elevation. These findings provide insight into the neuroprotective effect of PDGF during the initial stages of ocular hypertensive injury, which could have important implications for the early detection and treatment of this sight-threatening disease.

## METHODS

### Animals

A total of 48 animals were used for this study. Adult 275 to 360 g male Sprague Dawley rats were purchased from Charles River (Margate, Kent, UK) and maintained in accordance with guidelines set forth by the UK Home Office regulations for the care and use of laboratory animals, the UK Animals (Scientific Procedures) Act (1986), and the Association for Research in Vision and Ophthalmology's Statement for the Use of Animals in Ophthalmic and Visual Research.

**Experimental Ocular Hypertension Model.** Raised IOP (ocular hypertension [OHT]) was induced using a modification of the method developed by Levkovitch-Verbin et al.<sup>19</sup> Rats were anesthetized with ketamine (50 mg/kg) and xylazine (10 mg/kg). Intraocular pressure was measured in both eyes using the TonoLab rebound tonometer (iCare, Tiolat Oy, Finland) within 5 minutes of the onset of anesthesia between the hours of 9:00 and 11:30 AM to minimize the influence of diurnal variation or general anesthesia on measured IOP.<sup>20</sup>

One eye was injected with 3  $\mu$ L of 0.5  $\mu$ g/ $\mu$ L; that is, 1.5  $\mu$ g PDGF-AB (#100-00AB; Peprotech, Rocky Hill, NJ, USA) or sterile PBS (Sigma-Aldrich Corp., St. Louis, MO, USA) using a 30-gauge needle mounted on a 5  $\mu$ L glass Hamilton syringe (Hamilton Bonaduz AG, Bonaduz, Switzerland). Solutions for injection were masked at the time of injection. The same eye then underwent translimbal laser photocoagulation using a diode laser (wavelength 532 nm, spot size 50  $\mu$ m, power 700 mW, duration 600 ms). The fellow untreated eye was used as a control.

Intraocular pressure of both eyes was rechecked 24 hours after the laser procedure under general anesthesia as described above, and again a week later. Animals with IOP of less than 20 mm Hg at 1 week following the initial laser treatment received another round of translimbal laser photocoagulation to the same eye. Animals also received a second intravitreal injection at this point, and were divided into groups of "saline-saline" (saline,  $n = 20$ ), "PDGF-saline" (PDGF  $\times$  1,  $n = 15$ ) or "PDGF-PDGF" (PDGF  $\times$  2,  $n = 13$ ). Intraocular pressure was recorded under general anesthesia the following day, 8 days after the first laser treatment. At 2 weeks after the original procedure, bilateral IOP was recorded again and the animals were culled for tissue processing.

An additional set of control experiments was performed on animals that received intravitreal saline injections without laser

photocoagulation (saline inj-no laser,  $n = 5$ ), laser photocoagulation without intravitreal injections (laser-no inj,  $n = 5$ ), laser photocoagulation with saline injections (laser with saline,  $n = 6$ ) and unlasered control eyes (control,  $n = 6$ ) for immunohistochemistry of retinal sections.

## Immunohistochemistry

**Retinal and Longitudinal ONH Sections.** Eyes were fixed with 4% paraformaldehyde for 30 minutes before being transferred to 30% sucrose in PBS (control,  $n = 6$ ; saline,  $n = 6$ ; PDGF  $\times$  1,  $n = 4$ ; PDGF  $\times$  2,  $n = 4$ ). Eyes then were immersed in embedding capsules with the plica semilunaris perpendicular to the plane of sectioning. Retina sections of 14  $\mu$ m thickness were collected through the dorsal-ventral/superior-inferior axis of the retina.

Slides were blocked in 10% normal goat serum (NGS) in PBS with 0.5% Triton X-100 for one hour at room temperature. Primary antibodies made up in buffer solution of 4% NGS in PBS with 0.3% Triton X-100 included antibodies against rabbit  $\beta$ III-tubulin (1:1000; Covance Research Products, Inc., Denver, NJ, USA), mouse  $\beta$ III-tubulin (1:2000; Promega, Madison, WI, USA), mouse NeuN (1:250; EMD Millipore, Billerica, MA, USA), mouse post-synaptic density protein 95 (PSD-95, 1:1000; Abcam, Cambridge, UK), chicken synaptophysin (SY38, 1:1000; Abcam), rabbit glutamate receptor-1 (GluR1, 1:50; Calbiochem, San Diego, CA, USA), guinea pig ionized calcium binding adaptor protein 1 (Iba-1; 1:500; Synaptic Systems, Göttingen, Germany), rabbit phospho-PDGF receptor  $\alpha$  (pPDGFR, 1:50; Abcam), rabbit CD45 (1:300; Abcam). Alexa-Fluor-conjugated secondary antibodies (1:1000; Invitrogen, Carlsbad, CA, USA) then were added for one hour together with 4',6-diamidino-2-phenylindole (DAPI) stain. Two slides also were stained in the absence of each primary antibody for use as negative controls.

Images were taken on a Leica SP5 confocal microscope at  $\times 40$  and  $\times 63$  magnification with z-step intervals of 0.3  $\mu$ m. Open-source image processing software Fiji<sup>21</sup> was used to reconstruct z-stack projections of individual optical sections for quantification. Images for the quantification of synaptic marker density in the inner plexiform layer (IPL) were taken from six images per eye using  $\times 40$  magnification at the area bounded by the RGC layer (RGCL) and inner nuclear layer (INL), with the stack end-points set to visualize 4',6-diamidino-2-phenylindole (DAPI)-stained nuclei at the RGCL. Only sections with the ONH clearly visible were chosen for analysis to ensure that the regions being assessed were equidistant from the ONH and along the superior-inferior axis, as far as possible. This is important, as topographical studies of rodent retinas have shown that the density of RGCs varies with distance from the ONH.<sup>22</sup> Confocal images were thresholded to the average of five positively-staining synaptic puncta for each channel, and counted using the automated Analyze Particle plug-in on Fiji which measured the total number of particles above the set threshold value. Only particles within the area bounded by the RGCL and INL (the IPL area) were counted. The z-stack volume was calculated by multiplying the z-step size by the number of slices per stack and the IPL area for each stack. The total particle count for all slices through the stack then was divided by the z-stack volume to obtain the synaptic density for each marker.

Retinal ganglion cell numbers were quantified based on the numbers of  $\beta$ III-tubulin and DAPI-positive cells within the RGC layer. Retinal regions used in this analysis were equidistant from the optic nerve head and taken from at least four individual sections per eye. Tubulin fluorescent intensity within the IPL also was assessed within this region by measuring the fluorescent integrated density within at least

eight  $30 \times 30 \mu\text{m}$  regions positioned between the RGCL and INL.

Differential levels of CD45 expression can be used to determine if Iba-1-positive cells are infiltrating monocytes from the peripheral circulation, which show high levels of CD45, or part of a resident microglial population that express CD45 at low levels.<sup>23</sup> Therefore, Iba-1-positive cells in retinal sections also were assessed for levels of CD45-expression and categorized as CD45<sup>hi</sup> or CD45<sup>lo</sup> based on the intensity of staining.

Analysis of longitudinal ONH sections focused on the lamina zone, which has been defined as a conical area bordered by the posterior sclera proximally and the start of the myelinated optic nerve distally.<sup>24,25</sup>

**Whole Mounts and Transverse ONH Sections.** Whole mount retinas (control,  $n = 5$ ; saline,  $n = 6$ ; PDGF  $\times 1$ ,  $n = 4$ ; PDGF  $\times 2$ ,  $n = 2$ ) were fixed in 4% paraformaldehyde and blocked in 5% NGS, 0.2% BSA, and PBS with 0.3% Triton X-100 for 1 hour with gentle shaking at room temperature based on a protocol suggested by Tual-Chalot et al. 2013.<sup>26</sup> Blocking solution then was replaced with primary antibodies (as above) made up in the same buffer at 4°C overnight and washed four times, 10 minutes each, in PBS with 0.3% Triton X-100 at room temperature. Secondary antibodies with DAPI were applied for four hours at room temperature with gentle shaking, and then washed four more times in PBS with 0.3% Triton X-100.

Confocal images of whole-mount retina Iba-1,  $\beta$ III-tubulin, and pPDGFR immunofluorescence were taken at  $\times 40$  magnification. Details of all treatment groups were masked at the time of assessment.

Transverse optic nerve sections were obtained from scleral cups after retinas had been removed for whole mount staining, and processed in a similar manner to the longitudinal ONH sections.

### Real-Time qPCR Reaction

RNA was extracted from retinas (control,  $n = 4$ ; saline,  $n = 5$ ; PDGF  $\times 1$ ,  $n = 4$ ; PDGF  $\times 2$ ,  $n = 4$ ) using the RNeasy Mini Kit (Qiagen Ltd., Manchester, UK) with on-column DNase digestion. Complementary DNA (cDNA) synthesis was performed using the SuperScript III First-Strand synthesis Supermix kit from Life Technologies, Inc. (Frederick, MD, USA). Taqman Gene Expression Assay primer/probes were used with TaqMan Fast Advanced Master Mix (both from Life Technologies, Inc.) for qPCR. Gene expression assays for *Arc* (Rn00571208\_g1), *Selp* (Rn00565416\_m1), *MCP-1* (Rn00580555\_m1), *CX3CR1* (Rn02134446\_s1), *IL-6* (Rn01410330\_m1), *IL-10* (Rn00563409\_m1), and *GAPDH* (Rn01775763\_g1) were purchased from Life Technologies, Inc. Between 30 and 50 ng cDNA in  $\leq 2 \mu\text{L}$  volume was used per reaction. The system was programmed to run for 40 cycles at the following settings: 50°C for 2 minutes, 95°C for 20 seconds, 95°C for 3 seconds, and 60°C for 30 seconds each, according to the suggested protocol from Applied Biosystems (Foster City, CA, USA). *GAPDH* was used as a reference gene, and the standard curve method was used for relative quantification of gene expression.

### Western Blotting

Retinas (control, saline, PDGF  $\times 1$ , PDGF  $\times 2$ ;  $n = 3$ ) were homogenized in complete lysis-M (Roche, Berlin, Germany) containing protease inhibitor (Roche) and phosphatase inhibitor (Thermo Fisher Scientific, Grand Island, NY, USA). Protein (10  $\mu\text{g}$ ) was loaded into 4–12% pre-cast gels (Life Technologies) and electro-transferred to PVDF membranes (Life Technologies). Membranes were blocked in 5% dried skimmed milk in PBS with 0.2% Tween20 (Sigma-Aldrich Corp.) for 1 hour and

incubated overnight with primary antibody in blocking solution at 4°C. Primary antibodies included PI3K (1:500; Cell Signaling, Herts, UK) and  $\beta$ -actin (1:1000; Cell Signaling) horseradish peroxidase (HRP) conjugated secondary antibodies (1:10,000; Vector Laboratories Ltd., Peterborough, UK) were used for 1 hour at 4°C before signal detection using ECL Prime (GE Healthcare, Amersham, UK) and an Alliance Western blot imaging system (UVItect Ltd., Cambridge, UK).

### Statistical Analysis

All data were expressed as mean  $\pm$  SEM. Differences in the mean level of IOP and cumulative IOP exposure in control and lasered eyes were tested for statistical significance using the unpaired *t*-test. A 1-way ANOVA with Bonferroni's multiple comparison test was performed for all other statistical analyses using Graphpad Prism v5.0b.

## RESULTS

### PDGF Increased IPL Synaptic Proteins and $\beta$ III-Tubulin Levels in Eyes With IOP Elevation

Cumulative IOP exposure measured over 2 weeks was significantly higher in eyes that received laser photocoagulation than in control eyes ( $P < 0.0001$ ): saline (lasered =  $360 \pm 111.5$ , control =  $172.2 \pm 15.34 \text{ mm Hg.days}$ ), PDGF  $\times 1$  (lasered =  $396.1 \pm 139$ , control =  $170.9 \pm 17.87 \text{ mm Hg.days}$ ), PDGF  $\times 2$  (lasered =  $439.6 \pm 125.3$ , control =  $174.1 \pm 21.64 \text{ mm Hg.days}$ ). No significant difference was found in IOP measurements amongst all laser treated eyes. Sixty to 75% of lasered eyes required subsequent re-treatment one week later, consistent with numbers cited from previous studies.<sup>19</sup> The mean IOP of eyes that underwent laser photocoagulation was higher than unlasered control eyes in all experimental groups (Supplementary Fig. S1).

Analysis of positive immunostained synaptic puncta in the IPL showed that the density of PSD-95, SY38, and GluR1 decreased with high IOP and saline injection (PSD-95 =  $4.59 \pm 0.41$ , SY38 =  $4.46 \pm 0.38$ , GluR1 =  $5.94 \pm 0.50$  puncta per  $\mu\text{m}^3$ ), compared to control eyes (PSD-95 =  $10.57 \pm 0.66$ , SY38 =  $7.46 \pm 0.28$ , GluR1 =  $14.36 \pm 1.27$  puncta per  $\mu\text{m}^3$ ; Fig. 1). However, eyes that had high IOP which were injected with PDGF showed a statistically significant increase in the levels of all 3 synaptic markers compared to the high IOP and saline injection group (PDGF  $\times 1$ : PSD-95 =  $8.65 \pm 0.43$ , SY38 =  $8.68 \pm 0.51$ , GluR1 =  $9.03 \pm 0.60$ ; PDGF  $\times 2$ : PSD-95 =  $9.56 \pm 0.61$ , SY38 =  $7.31 \pm 0.39$ , GluR1 =  $11.84 \pm 0.60$  puncta per  $\mu\text{m}^3$ ; Fig. 1). Immunohistochemical images for PDGF  $\times 1$  have been omitted from the Figures due to space constraints.

*Arc*, which encodes the activity-regulated cytoskeleton-associated protein, is an immediate early gene that is involved closely with modulating synaptic changes in the central nervous system.<sup>27–29</sup> A significant increase in *Arc* mRNA was observed in eyes with high IOP following PDGF  $\times 1$  administration ( $6.92 \pm 3.71$ -fold/control) in comparison with the saline group ( $1.46 \pm 0.31$ -fold/control). Two treatments of PDGF in hypertensive eyes showed only a modest effect on *Arc* mRNA ( $2.69 \pm 0.50$ -fold/control), although synaptic density in the IPL was comparable to the levels detected with PDGF  $\times 1$ .

Changes in synaptic density were not a result of a difference in RGC survival between groups as no significant decrease was detected in the number of  $\beta$ III-tubulin-positive RGCL cells at 2 weeks after laser-induced OHT (Fig. 2). However, the intensity of  $\beta$ III-tubulin was significantly decreased in the IPL of eyes with elevated IOP that received only saline injections ( $0.71 \pm 0.02$ -fold/control versus PDGF  $\times 1$  =  $1.04 \pm 0.08$ , PDGFX2 =



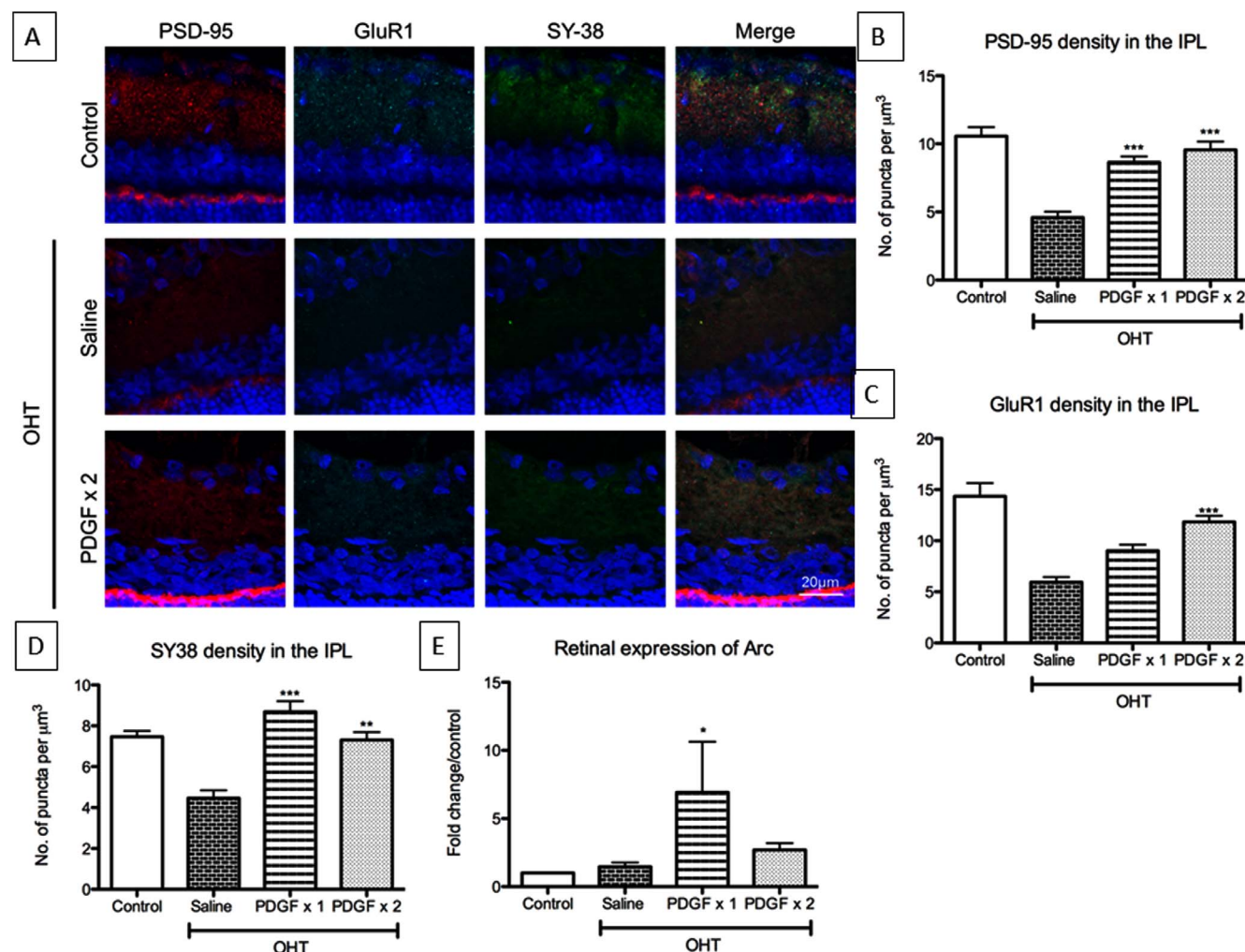


**FIGURE 1.** (A–D) Ocular hypertensive eyes (OHT) that received saline injections showed a decrease in synaptic proteins PSD-95, GluR1, and SY38 in the IPL relative to control. However, OHT eyes that had been treated with PDGF showed a significant increase in these proteins in comparison with vehicle-injected eyes. (E) mRNA levels of *Arc* were significantly elevated in eyes with high IOP that had been treated with one injection of PDGF. A 1-way ANOVA was performed for PDGF-treated against saline-only eyes. \*\* $P < 0.01$ , \*\*\* $P < 0.001$ . Error bars: SEM.

$0.95 \pm 0.05$ -fold/control; Fig. 2) indicating a possible loss of RGC dendrites that occurred before cell death.

Animals that received intravitreal injections of saline alone without laser photocoagulation did not show any significant difference from unlesioned control eyes, while intravitreal injections of saline with laser photocoagulation showed a similar effect as laser photocoagulation alone (Supplementary Fig. S2) suggesting that saline alone did not contribute to the observed synaptic changes.

### Activated PDGF Receptor Strongly Colocalized With Iba-1+ Cells in the Retina

Immunohistochemical analysis of whole mount and sectioned retinas revealed only moderate colabeling of p-PDGFR with the RGC markers  $\beta$ III-tubulin and NeuN (Fig. 3). However, strong colocalization was noted between Iba-1-positive cells and activated PDGF receptors. This was particularly marked in eyes with ocular hypertension, which showed high numbers of Iba-1-positive cells (Fig. 4).

The PI3K pathway, which has an important role in PDGF-mediated neuroprotection,<sup>1</sup> was significantly increased after two doses of intravitreal PDGF ( $0.76 \pm 0.07$  OD) relative to

control ( $0.43 \pm 0.05$  OD) or saline ( $0.36 \pm 0.02$  OD) groups. A single injection of PDGF also showed an increase in signaling activity ( $0.67 \pm 0.12$  OD) although this did not reach statistical significance.

### Effect of PDGF on the Inflammatory Milieu Within the Retina and Optic Nerve

Differential CD45 expression has been used previously to distinguish between infiltrating monocytes and resident microglial populations.<sup>23,30</sup> To validate this distinction in the eye, a longitudinal section through a normal optic nerve and adjacent posterior ciliary vessel was stained for CD45 and Iba-1 (Supplementary Fig. S3). This showed intense expression of CD45 on circulating monocytes in the blood vessel (CD45<sup>hi</sup>), while CD45 immunostaining was only minimally present in Iba-1-positive myeloid cells within the optic nerve (CD45<sup>lo</sup>).

Platelet-derived growth factor-treated ocular hypertensive eyes had increased numbers of Iba-1+/CD45<sup>lo</sup> (PDGF  $\times$  1 =  $8.16 \pm 1.34$ , PDGF  $\times$  2 =  $5.16 \pm 1.11$ -fold change/control) and Iba-1+/CD45<sup>hi</sup> cells in the retina, relative to eyes with elevated IOP that had only received saline injections ( $1.61 \pm 0.35$ -fold change/control; Fig. 4). The increase in Iba-1+/CD45<sup>hi</sup> cells

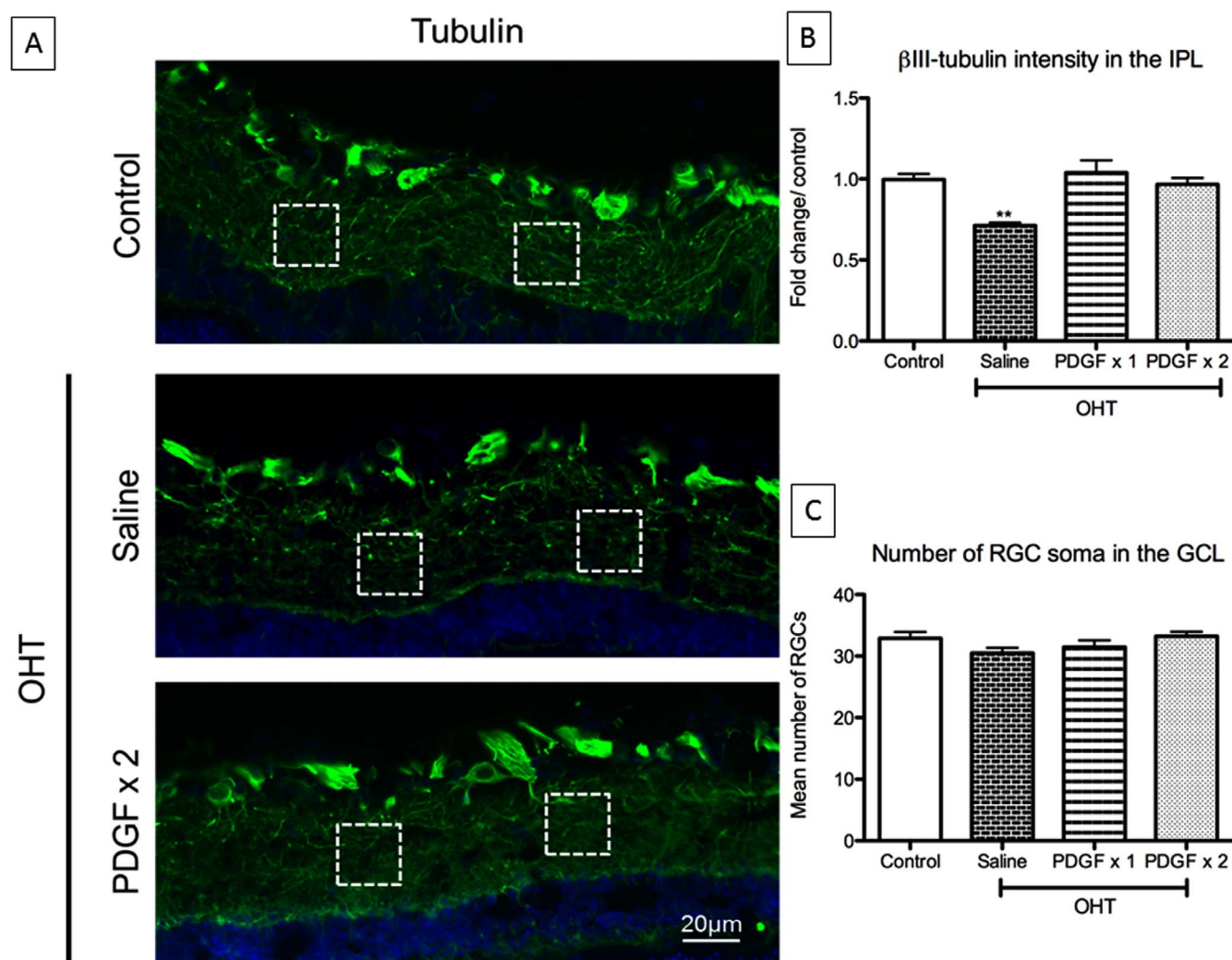


**FIGURE 2.** (A) Platelet-derived growth factor prevented the loss of βIII-tubulin staining in the inner plexiform layer of eyes with elevated IOP (B) Eyes that were injected with saline showed a significant decrease in βIII-tubulin intensity in the IPL compared to control, while eyes that received PDGF treatment did not. (C) No loss of RGC cell number was seen 2 weeks after elevated IOP in any of the groups. \*\* $P < 0.01$ .

with PDGF injections was much higher (saline =  $2.67 \pm 0.73$  versus PDGF  $\times 1 = 29.44 \pm 2.78$ , PDGF  $\times 2 = 26.56 \pm 6.56$ -fold change/control) in comparison with the changes seen in Iba-1+/CD45<sup>lo</sup> cells.

Real-time PCR analysis of *Selp*, which codes for p-selectin, also was elevated in the retina of eyes that had received single PDGF injections ( $26.8 \pm 14.12$ -fold change/control) in comparison with saline-injected eyes ( $2.89 \pm 1.07$ -fold change/control). Expression of monocyte chemoattractant protein-1 (MCP-1) showed a very similar trend in eyes with single PDGF ( $6.43 \pm 1.52$ -fold change/control) injections in comparison with saline-injected eyes ( $1.52 \pm 0.27$ -fold change/control). Eyes that were injected with PDGF twice showed higher levels of both *selp* and MCP-1, although this did not reach statistical significance ( $9.41 \pm 5.70$  and  $3.65 \pm 0.39$ -fold change/control, respectively). Both P-selectin and MCP-1 have important roles in mediating monocyte transmigration through blood vessels,<sup>31,32</sup> providing further support for the increased numbers of Iba-1+/CD45<sup>hi</sup> cells that were detected in retinas of OHT eyes treated with PDGF.

Examination of the ONH showed an increase in only Iba1+/CD45<sup>lo</sup> (saline =  $1.44 \pm 0.13$  versus PDGF  $\times 1 = 2.23 \pm 0.18$ , PDGF  $\times 2 = 2.18 \pm 0.15$ -fold change/control; Fig. 5) but not Iba1+/CD45<sup>hi</sup> cells under similar conditions (data not shown).

### PDGF Alters Inflammatory Cytokine Production in the Retina

Real-time PCR analysis of retinal tissues detected an increase in the microglial marker *CX3CR1* in PDGF-treated eyes relative to saline-injected eyes with high IOP, which may be related to the increased numbers of microglia and monocytes detected in the retina, although this did not reach statistical significance (Fig. 6). Expression of the anti-inflammatory cytokine *IL-10* also was higher in ocular hypertensive eyes that received PDGF injections (PDGF  $\times 1 = 5.43 \pm 0.47$ , PDGF  $\times 2 = 4.88 \pm 1.31$ -fold change/control) compared to saline ( $2.51 \pm 0.67$ -fold change/control), while the reverse trend was noted with *IL-6* (saline =  $12.51 \pm 3.45$  versus PDGF  $\times 1 = 5.40 \pm 1.80$ , PDGF  $\times 2 = 5.78 \pm 2.24$ -fold change/control).

### DISCUSSION

Platelet-derived growth factor has been demonstrated previously to provide robust axonal protection and prevent cell death in RGCs using an experimental model of ocular hypertension.<sup>1</sup> The results of our study provided new evidence that PDGF may promote RGC dendrite health and synaptic



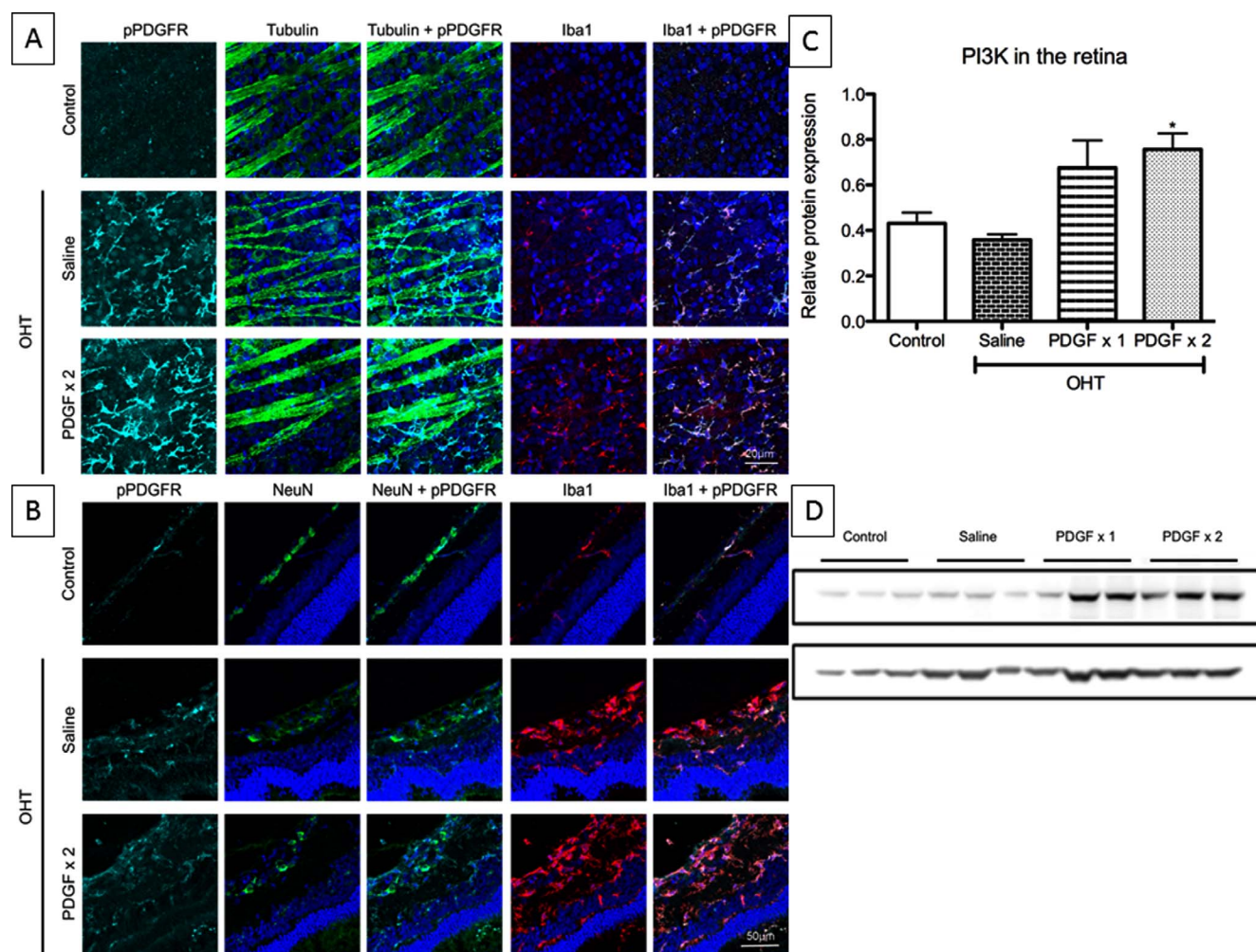


FIGURE 3. Phosphorylated PDGF receptor (teal) showed only moderate costaining with RGC markers  $\beta$ III-tubulin and NeuN (green) in retinal wholemounts (A) and sections (B), while intense colocalization was noted with Iba-1 positive cells (red). (C, D) PI3K signaling was increased in eyes that received PDGF injections, in comparison with control and saline-injected eyes. \* $P < 0.05$ .

density in ocular hypertensive eyes. These changes appear to be associated with marked alterations in the inflammatory cell populations within the retinal and optic nerve head, which could facilitate neuron-glia interactions that help to mediate this neuroprotective effect.

Changes to RGC synapses and dendrites are thought to be early events in experimental glaucoma.<sup>18,33</sup> Our study supports these findings where reductions in postsynaptic density markers PSD-95 and GluR1 as well as the synaptic vesicle-associated protein SY38 were found in eyes with elevated IOP. Interestingly, treatment with PDGF resulted in significantly higher levels of all 3 synaptic proteins as well as the immediate early gene *Arc*, which has an active role in modulating dendritic structure and function as well as synaptic plasticity.<sup>27–29</sup> As the majority of ocular hypertensive eyes were subjected to two consecutive lasers in each treatment group, varying exposure to laser photocoagulation alone is unlikely to account for the significant differences in experimental outcomes. Two injections of PDGF appeared to result in lower *Arc* expression than a single dose, although a possible explanation for this discrepant effect could be feedback downregulation of gene expression. Our observations that twice as much PDGF administration appeared to result in downregulation of *Selp* and *MCP-1* also may be related to the heightened production of matrix metalloproteinases and

fibroblast growth factor-2, which have been shown to reduce transendothelial cell migration.<sup>34–36</sup> Further studies must be conducted to verify this.

Whether PDGF directly influences the synaptodendritic compartment of RGCs, or if it acts through an intermediary cell-type remains unclear. An earlier study demonstrated that PDGF increases *Arc* expression in cortical neurons via Egr-1 activation from the MAPK/ERK pathway<sup>37</sup> suggesting that PDGF could have a similar direct effect on RGCs. This could be related to the increased retinal activation of PI3K induced by PDGF observed in our experiments. A pertinent finding of our study was that PDGF treatment also caused marked changes in resident microglial (Iba-1/CD45<sup>lo</sup>) as well as infiltrating monocyte-derived macrophage (Iba-1/CD45<sup>hi</sup>) populations in the eye. These findings support results from Bethel-Brown et al.<sup>7</sup> who showed that PDGF is a potent chemoattractor for monocytes via MCP-1 signaling. Platelet-derived growth factor receptor  $\alpha$  has been found on monocytes and macrophages within the CNS,<sup>38,39</sup> and prominently colocalized with Iba-1 cells in the retina following intravitreal PDGF injections in our study. This raises the intriguing possibility of an association between PDGF-induced alterations in microglial/macrophagic activity and synaptic plasticity in our experiments. Furthermore, the site-specific differences that we noted in the microglial response to PDGF at the retina and ONH may be

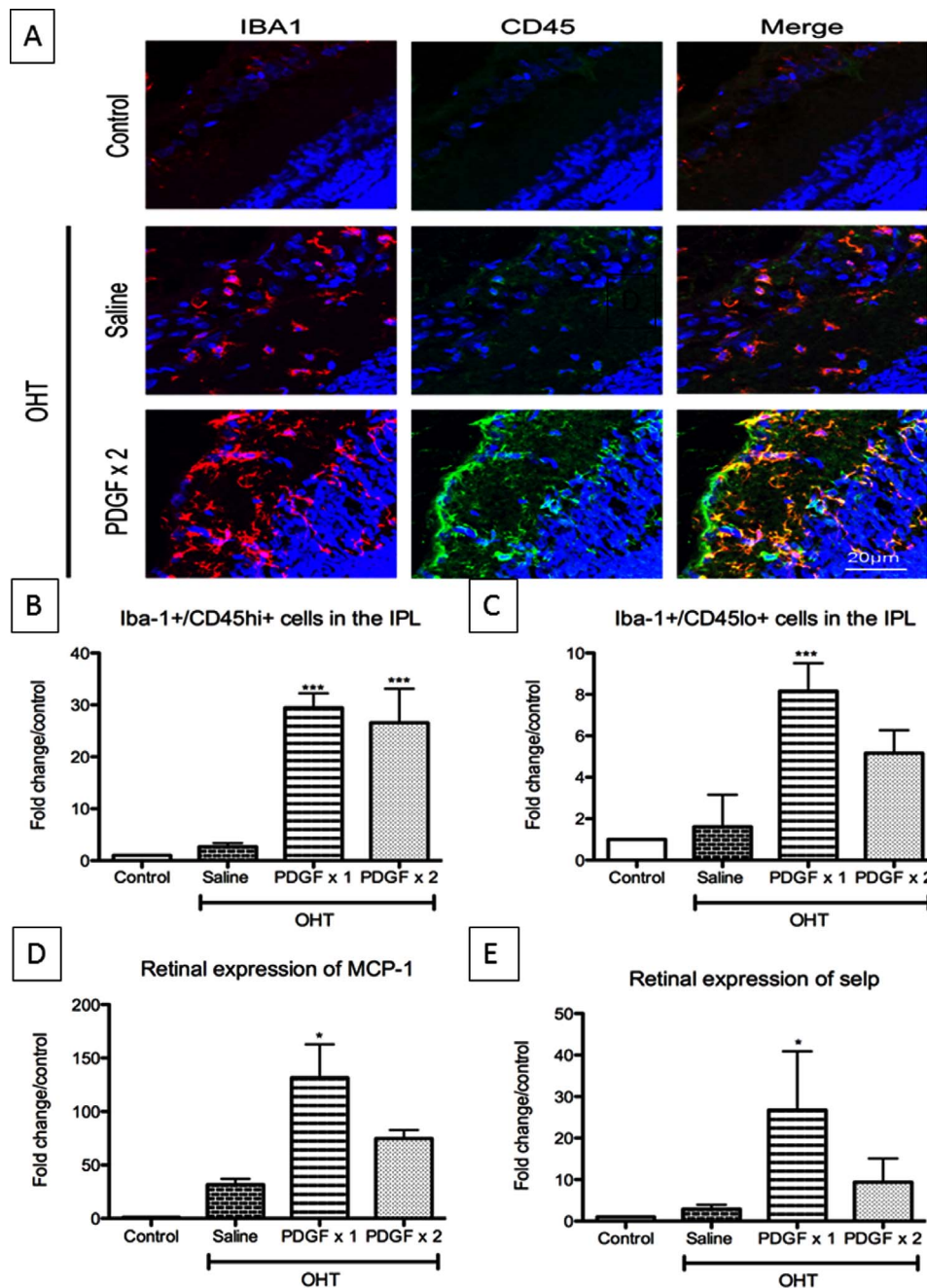


**FIGURE 4.** (A) Ocular hypertensive eyes that were injected with PDGF showed an increase in Iba-1+/CD45<sup>hi</sup> (bright green) (B) and Iba-1+ (red) / CD45<sup>lo</sup> (light green) (C) cell populations in the retina. We used DAPI to stain cell nuclei (blue). QPCR of retinal tissue for MCP-1 (D) and the p-selectin gene *selp* (E) also were shown to be higher in PDGF-treated eyes than saline only eyes with high IOP. \* $P < 0.05$ , \*\* $P < 0.01$ , \*\*\* $P < 0.001$ .

relevant to the mechanism of action of PDGF as the recruitment of leukocytes is believed to be largely confined to postcapillary endothelium in the ganglion cell, nerve fiber and inner nuclear layers.<sup>40,41</sup> This would suggest that the synapse preserving effect of PDGF is largely confined to the retina, and unlikely to involve larger vessels at the ONH.

There is strong evidence of an association between microglial activation and RGC loss in experimental glaucoma. Inactivation of microglia appears to have a beneficial effect on RGC survival,<sup>42</sup> while deficiencies in fractalkine, which normally inhibits microglial activity, produce the converse outcome of exacerbating RGC death instead.<sup>43</sup> Interestingly, however, enhanced neuroprotection has been demonstrated in

parallel with increased numbers of Iba-1-positive cells in the retina, following intravitreal injections of ciliary neurotrophic factor (CNTF) or hepatocyte growth factor (HGF) after optic nerve transection.<sup>44</sup> These findings support our own observations with PDGF treatment in an OHT model of glaucoma. It is clear that further research into characterizing the inflammatory profiles of different optic nerve injury models is necessary to deepen our understanding of how this influences neuron-glia interactions.

Our results also are in keeping with a study by London et al.<sup>45</sup> who elegantly demonstrated that enhancing the infiltration of monocyte-derived macrophages into glutamate-intoxicated retinas resulted in a switch in the behavior of the local



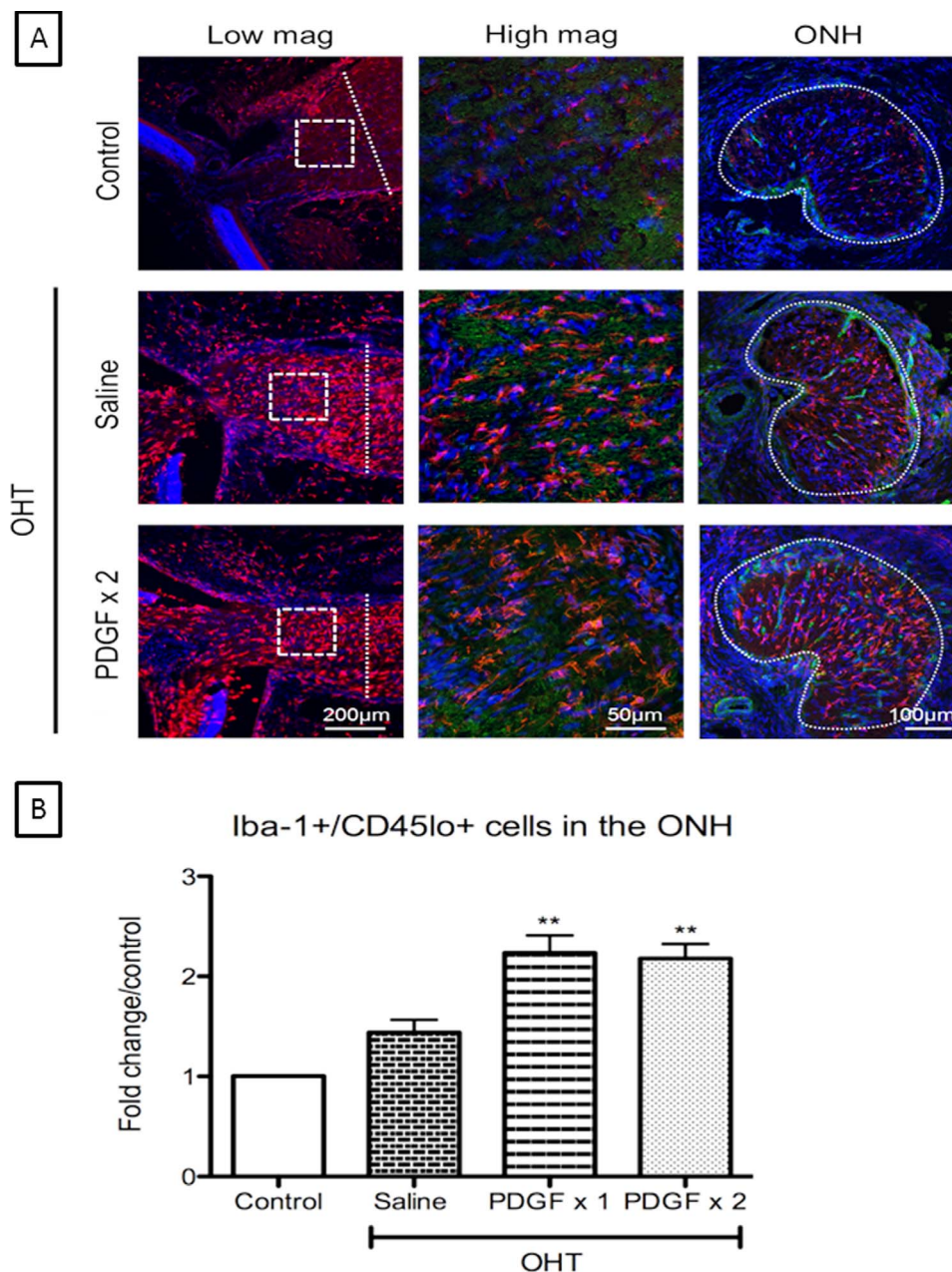
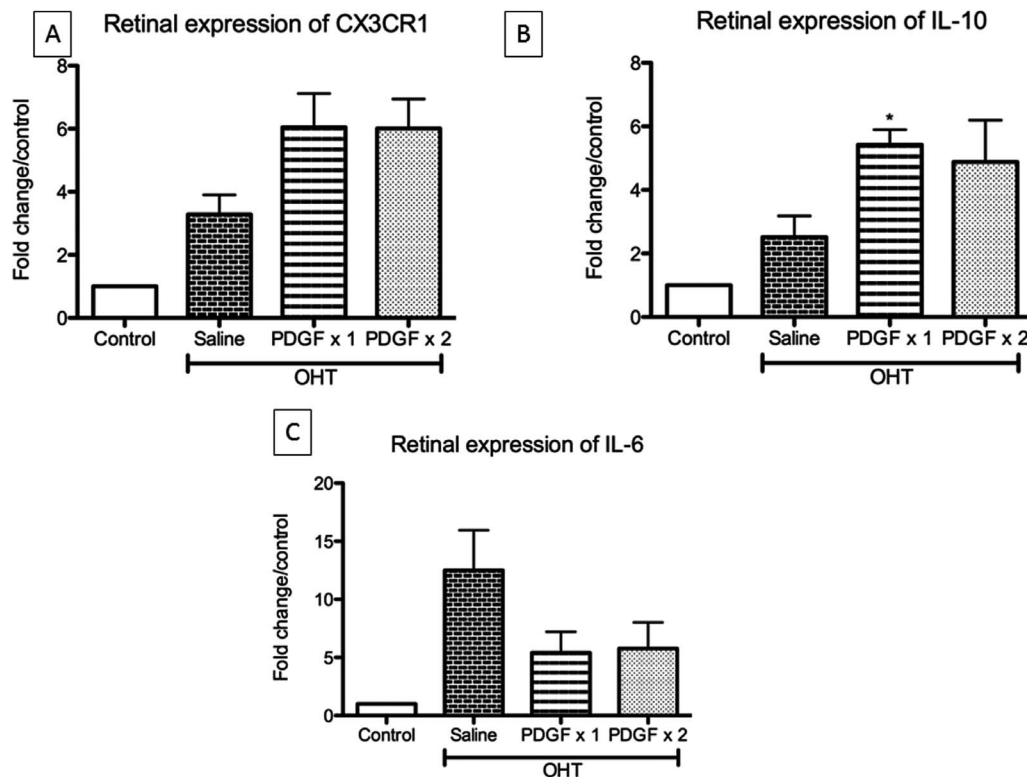


FIGURE 5. (A, B) Optic nerve head sections showed higher numbers of Iba-1+/CD45<sup>lo</sup> cells alone. \* $P < 0.05$ , \*\* $P < 0.01$ , \*\*\* $P < 0.001$ .

inflammatory milieu from a proinflammatory to an anti-inflammatory state. This effect was at least partially dependent on IL-10 production, which also was increased in our experimental groups that received PDGF treatment. Furthermore, IL-10 has been suggested to have a dominant role in microglia-induced synaptic remodeling,<sup>46</sup> which could provide additional support for our findings. This contrasts with a previous study where radiation treatment was suggested to be neuroprotective in the DBA/2J mouse model of glaucoma, due to the elimination of monocytic transmigration into the optic nerve head.<sup>30</sup> However, a subsequent study that examined a rat model of ocular hypertension found that there was no difference in RGC survival or Iba-1 cell density following ocular radiation.<sup>47</sup> The same study also reported an absence of monocyte entry into the ONH with elevated IOP, consistent with our results.

Microglia are believed to be intimately involved in the modulation of synaptic density in physiological and pathologic states in the CNS,<sup>13,16</sup> although to our knowledge ours is the first study to show that higher numbers of microglia and monocyte-derived macrophages may be associated with increased synaptic density within the retina. Microglia<sup>48</sup> and monocytes<sup>49</sup> produce high levels of brain-derived neurotrophic factor (BDNF), which is known to be a potent modulator of synapses throughout the CNS.<sup>50,51</sup> Thus, higher numbers of these cell-types resulting in greater BDNF secretion could contribute to increased synaptic density. Another important consideration is the fact that retinal glia do not act in isolation, but are perpetually engaged in a wide range of dynamic interactions with other cell types. Therefore, it is possible that the alterations in microglia and macrophages observed in our experiments also induced changes in astrocytes and Müller glia, which have important roles in regulating neuronal health.





**FIGURE 6.** Treatment of high IOP eyes with PDGF resulted in an increase in (A) CX3CR1 and (B) IL-10 mRNA in the retina, although this only reached statistical significance for the latter. (C) Interleukin-6 was detected at lower levels in PDGF-injected eyes with high IOP, relative to saline-only eyes. \* $P < 0.05$ .

A deeper understanding of these cellular interactions would no doubt be valuable in identifying potential pathways to protect RGCs from glaucomatous injury.

The laser-induced ocular hypertension model has been extensively used in previous studies and has the advantage of a rapid and reliable elevation of IOP in most treated animals. The clearly defined onset of injury in this model allows the time-course of early pathologic changes in RGC after IOP elevation to be studied. However, the model has several important limitations relevant to the interpretation of the results of the current study. Many of the eyes in the experimental group were relasersed after 1 week to increase the IOP (Supplementary Fig. S1). The criterion for relasering was IOP  $< 20$  mm Hg at 1 week and in this regard there was some variation between groups. This issue potentially complicates separation of the effects of laser-induced inflammation from the effects of laser-induced IOP elevation. There also was some variability in the rate of IOP increase and the duration of IOP elevation in different animals. Although this variation did not result in significant differences in cumulative IOP, previously identified as the IOP parameter correlated most strongly with RGC loss in the laser model,<sup>19,52</sup> there was at least a trend towards higher IOP at 1 week in PDGF-treated eyes which should be taken into account when interpreting the results since early exposure to higher IOP alone could have resulted in greater microglial/monocytic recruitment and activation. It also is possible that some differences in IOP profile between groups could have been missed with the IOP measurement time-points used. In future studies we plan to compare the results in the laser model of ocular hypertension to other models, including a microbead injection model of ocular hypertension in which we expect induced inflammation to be less of a confounding issue.<sup>53,54</sup> Awake IOP measurements will

enable more frequent measurement of IOP and, thus, more complete IOP profiles for individual animals.

To the best of our knowledge, this is the first study to suggest that PDGF promotes synaptic density in the retina of ocular hypertensive eyes. Further work must be done to evaluate whether the increase in microglia and monocyte-derived macrophage populations associated with PDGF treatments are directly responsible for this effect, although current literature would seem to support this hypothesis. Defining the biological pathways that underlie synaptic changes occurring in the initial stages of glaucoma would provide important insights into the pathogenesis of this disease, and may lead to potential opportunities for early therapeutic intervention.

### Acknowledgments

The authors thank Tin Aung Tun (Singapore Eye Research Institute) for his technical assistance.

Supported by the Agency for Science Technology and Research Singapore (RC), the Cambridge Eye Trust, the HB Allen Charitable Trust and the Jukes Glaucoma Research Fund, and by Grant 1868 from Fight for Sight (KM).

Disclosure: **R.S. Chong**, None; **A. Osborne**, None; **R. Conceição**, None; **K.R. Martin**, None

### References

- Johnson TV, DeKorver NW, Levasseur VA, et al. Identification of retinal ganglion cell neuroprotection conferred by platelet-derived growth factor through analysis of the mesenchymal stem cell secretome. *Brain*. 2014;137:1-17.
- Tseng HC, Dichter MA. Platelet-derived growth factor-BB pretreatment attenuates excitotoxic death in cultured hippocampal neurons. *Neurobiol Dis*. 2005;19:77-83.

3. Zheng L-S, Ishii Y, Zhao Q-L, Kondo T, Sasahara M. PDGF suppresses oxidative stress induced  $Ca^{2+}$  overload and calpain activation in neurons. *Oxid Med Cell Longev*. 2013;2013:1-8.
4. Biswas SK, Zhao Y, Nagalingam A, Gardner TW, Sandrasegaran L. PDGF- and insulin/IGF-1-specific distinct modes of class IA PI 3-kinase activation in normal rat retinas and RGC-5 retinal ganglion cells. *Invest Ophthalmol Vis Sci*. 2008;3687-3698.
5. Kanamoto T, Rimayanti U, Okumichi H, Kiuchi Y. Platelet-derived growth factor receptor alpha is associated with oxidative stress-induced retinal cell death. *Curr Eye Res*. 2011;36:336-340.
6. Norazit A, Nguyen MN, Dickson CGM, et al. Vascular endothelial growth factor and platelet derived growth factor modulates the glial response to a cortical stab injury. *Neuroscience*. 2011;192:652-660.
7. Bethel-Brown C, Yao H, Hu G, Buch S. Platelet-derived growth factor (PDGF)-BB-mediated induction of monocyte chemoattractant protein 1 in human astrocytes: implications for HIV-associated neuroinflammation. *J Neuroinflamm*. 2012;9:1-1.
8. Nicholas RSJ, Wing MG, Compston A. Nonactivated microglia promote oligodendrocyte precursor survival and maturation through the transcription factor NF- $\kappa$ B. *Eur J Neurosci*. 2001;13:959-967.
9. Semple BD, Kossmann T, Morganti-Kossmann MC. Role of chemokines in CNS health and pathology: a focus on the CCL2/CCR2 and CXCL8/CXCR2 networks. *J Cereb Blood Flow Metab*. 2009;30:459-473.
10. Paolicelli RC, Bolasco G, Pagani F, et al. Synaptic pruning by microglia is necessary for normal brain development. *Science*. 2011;333:1456-1458.
11. Schafer DP, Lehrman EK, Kautzman AG, et al. Microglia sculpt postnatal neural circuits in an activity and complement-dependent manner. *Neuron*. 2012;74:691-705.
12. Perry VH, Nicoll JAR, Holmes C. Microglia in neurodegenerative disease. *Nat Rev Neurol*. 2010;6:193-201.
13. Wake H, Moorhouse AJ, Jinno S, Kohsaka S, Nabekura J. Resting microglia directly monitor the functional state of synapses in vivo and determine the fate of ischemic terminals. *J Neurosci*. 2009;29:3974-3980.
14. Bosco A, Steele MR, Vetter ML. Early microglia activation in a mouse model of chronic glaucoma. *J Comp Neurol*. 2001;519:599-620.
15. Ebner A, Casson RJ, Wood JPM, Chidlow G. Microglial activation in the visual pathway in experimental glaucoma: spatiotemporal characterization and correlation with axonal injury. *Invest Ophthalmol Vis Sci*. 2010;51:6448-6460.
16. Stevens B, Allen NJ, Vazquez LE, et al. The classical complement cascade mediates CNS synapse elimination. *Cell*. 2007;131:1164-1178.
17. Frankfort BJ, Khan AK, Tse DY, et al. Elevated intraocular pressure causes inner retinal dysfunction before cell loss in a mouse model of experimental glaucoma. *Invest Ophthalmol Vis Sci*. 2013;54:762-770.
18. Santina Della L, Inman DM, Lupien CB, Horner PJ, Wong ROL. Differential progression of structural and functional alterations in distinct retinal ganglion cell types in a mouse model of glaucoma. *J Neurosci*. 2013;33:17444-17457.
19. Levkovitch-Verbin H, Quigley HA, Martin KRG, Valenta D, Baumrind LA, Pease ME. Translimbal laser photocoagulation to the trabecular meshwork as a model of glaucoma in rats. *Invest Ophthalmol Vis Sci*. 2002;43:402-410.
20. Jia L, Cepurna WO, Johnson EC, Morrison JC. Effect of general anesthetics on iop in rats with experimental aqueous outflow obstruction. *Invest Ophthalmol Vis Sci*. 2000;41:3415-3419.
21. Schindelin J, Arganda-Carreras I, Frise E, et al. Fiji: an open-source platform for biological-image analysis. *Nat Methods*. 2012;9:676-682.
22. Salinas-Navarro M, Mayor-Torroglosa S, Jiménez-López M, et al. A computerized analysis of the entire retinal ganglion cell population and its spatial distribution in adult rats. *Vision Res*. 2009;49:115-126.
23. D'Mello C, Le T, Swain MG. Cerebral microglia recruit monocytes into the brain in response to tumor necrosis factor signaling during peripheral organ inflammation. *J Neurosci*. 2009;29:2089-2102.
24. Morrison J, Farrell S, Johnson EC, Deppmeier L, Moore CG, Grossman E. Structure and composition of the rodent lamina cribrosa. *Exp Eye Res*. 1995;60:127-135.
25. Hildebrand C, Remahl S, Waxman SG. Axo-glial relations in the retina-optic nerve junction of the adult rat: electron-microscopic observations. *J Neurocytol*. 1985;14:597-617.
26. Tual-Chalot S, Allinson KR, Fruttiger M, Arthur HM. Whole mount immunofluorescent staining of the neonatal mouse retina to investigate angiogenesis in vivo. *J Vis Exp*. 2013;77:e50546.
27. Bramham CR, Worley PF, Moore MJ, Guzowski JF. The immediate early gene *arc/arg3.1*: regulation, mechanisms, and function. *J Neurosci*. 2008;28:11760-11767.
28. Chowdhury S, Shepherd JD, Okuno H, et al. Arc interacts with the endocytic machinery to regulate AMPA receptor trafficking. *Neuron*. 2006;52:445-459.
29. Vazdarjanova A, McNaughton BL, Barnes CA, Worley PF, Guzowski JF. Experience-dependent coincident expression of the effector immediate-early genes. *J Neurosci*. 2002;22:10067-10071.
30. Howell GR, Soto I, Zhu X, et al. Radiation treatment inhibits monocyte entry into the optic nerve head and prevents neuronal damage in a mouse model of glaucoma. *J Clin Invest*. 2012;122:1246-1261.
31. Piccio L, Rossi B, Laudanna C, et al. Molecular mechanisms involved in lymphocyte recruitment in inflamed brain microvessels: critical roles for P-selectin glycoprotein ligand-1 and heterotrimeric G(i)-linked receptors. *J Immunol*. 2002;168:1940-1949.
32. Weyrich AS, McIntyre TM, McEver RP, Prescott SM, Zimmermann GA. Monocyte tethering by P-selectin regulates monocyte chemotactic protein-1 and tumor necrosis factor- $\alpha$  secretion. *J Clin Invest*. 1995;95:2297-2303.
33. Weber A, Harman C. Structure-function relations of parasol cells in the normal and glaucomatous primate retina. *Invest Ophthalmol Vis Sci*. 2005;46:1-11.
34. Favreau C, Preece G, Ager A. Transendothelial migration of lymphocytes across high endothelial venules into lymph nodes is affected by metalloproteinases. *Blood*. 2001;98:688-695.
35. Figueiredo C, Pais T, Gomes J, Chatterjee S. Neuron-microglia crosstalk up-regulates neuronal FGF-2 expression which mediates neuroprotection against excitotoxicity via JNK1/2. *J Neurochem*. 2008;107:73-85.
36. Zhang H, Issekutz AC. Down-modulation of monocyte trans-endothelial migration and endothelial adhesion molecule expression by fibroblast growth factor: reversal by the anti-angiogenic agent SU6668. *Am J Pathol*. 2002;160:2219-2230.
37. Peng F, Yao H, Bai X, et al. Platelet-derived Growth Factor-mediated induction of the synaptic plasticity gene *arc/Arg3.1*. *J Biol Chem*. 2010;285:21615-21624.
38. Miyata T, Toho T, Nonoguchi N, et al. The roles of platelet-derived growth factors and their receptors in brain radiation necrosis. *Radiat Oncol*. 2014;9:51.
39. Heldin C-H, Westermark B. Mechanism of action and in vivo role of platelet-derived growth factor. *Physiol Rev*. 1999;79:1283-1316.
40. Granger DN, Kubes P. The microcirculation and inflammation: modulation of leukocyte-endothelial cell adhesion. *J Leukoc Bio*. 1994;55:662-675.



41. Hayrer S. Acute retinal arterial occlusive disorders. *Prog Retin Eye Res.* 2011;30:359–394.
42. Bosco A, Inman DM, Steele MR, et al. Reduced retina microglial activation and improved optic nerve integrity with minocycline treatment in the DBA/2J mouse model of glaucoma. *Invest Ophthalmol Vis Sci.* 2008;49:1437–1446.
43. Wang K, Peng B, Lin B. Fractalkine receptor regulates microglial neurotoxicity in an experimental mouse glaucoma model. *Glia.* 2014;62:1943–1954.
44. Wong WK, Cheung AW, Yu SW, et al. Hepatocyte growth factor promotes long-term survival and axonal regeneration of retinal ganglion cells after optic nerve injury: comparison with CNT and BDNF. *CNS Neurosci Ther.* 2014;20:916–929.
45. London A, Itskovich E, Benhar I, et al. Neuroprotection and progenitor cell renewal in the injured adult murine retina requires healing monocyte-derived macrophages. *J Exp Med.* 2011;208:23–39.
46. Lim SH, Park E, You B, et al. Neuronal synapse formation induced by microglia and interleukin 10. *PLoS One.* 2013;8:e81218.
47. Johnson EC, Cepurna W, Choi D, Choe TE, Morrison JC. Radiation pretreatment does not protect the rat optic nerve from elevated intraocular pressure-induced injury. *Invest Ophthalmol Vis Sci.* 2015;56:412–419.
48. Ferrini F, De Koninck Y. Microglia control neuronal network excitability via BDNF signalling. *Neural Plast.* 2013;2013:429815.
49. Kerschensteiner M, Gallmeier E, Behrens L, et al. Activated human T cells, B cells and monocytes produce brain-derived neurotrophic factor in vitro and in inflammatory brain lesions: a neuroprotective role of inflammation? *J Exp Med.* 1999;189:865–870.
50. Parkhurst CN, Yang G, Ninan I, et al. Microglia promote learning-dependent synapse formation through brain-derived neurotrophic factor. *Cell.* 2013;155:1596–1609.
51. Kang H, Schuman EM. Long-lasting neurotrophin-induced enhancement of synaptic transmission in the adult hippocampus. *Science.* 1995;267:1658–1662.
52. Morrison JC, Johnson EC, Cepurna W, Jia L. Understanding mechanisms of pressure-induced optic nerve damage. *Prog Retin Eye Res.* 2005;24:217–240.
53. Sappington RM, Carlson BJ, Crish SD, et al. The microbead occlusion model: a paradigm for induced ocular hypertension in rats and mice. *Invest Ophthalmol Vis Sci.* 2010;51:207–216.
54. Samsel PA, Kisiswa L, Erichsen JT, et al. A novel method for the induction of experimental glaucoma using magnetic microspheres. *Invest Ophthalmol Vis Sci.* 2011;52:1671–1675.